[CANCER RESEARCH 62, 1205–1212, February 15, 2002]

Overexpression of Copper Zinc Superoxide Dismutase Suppresses Human Glioma Cell Growth[1]

Ying Zhang, Weiling Zhao, Hannah J. Zhang, Frederick E. Domann, and Larry W. Oberley[2]

Free Radical and Radiation Biology Program, Department of Radiation Oncology, B180 Medical Laboratories, College of Medicine, The University of Iowa, Iowa City, Iowa 52242

ABSTRACT

Copper zinc superoxide dismutase (CuZnSOD) is an essential primary antioxidant enzyme that converts superoxide radical to hydrogen peroxide and molecular oxygen in the cytoplasm. Cytosolic glutathione peroxidase (GPx) converts hydrogen peroxide into water. The overall goal of the present study was to explore the possible role of the antioxidant enzyme CuZnSOD in expression of the malignant phenotype. We hypothesized that overexpression of CuZnSOD would lead to the suppression of at least part of the human malignant phenotype. To test this hypothesis, human CuZnSOD cDNA was transfected into U118-9 human malignant glioma cells. CuZnSOD activity levels increased 1.5-, 2.0-, 2.6-, and 3.5-fold, respectively, in four stable transfected cell lines compared with wild type and vector controls. Overexpression of CuZnSOD altered cellular antioxidant enzyme profiles, including those of manganese superoxide dismutase, catalase, and GPx. The transfected clone with the highest CuZnSOD:GPx ratio (3.5) showed a 42% inhibition of tumor cell growth *in vitro*. The decreased rate of tumor cell growth *in vitro* was strongly correlated with the enzyme activity ratio of CuZnSOD:GPx. Glioma cells that stably overexpressed CuZnSOD demonstrated additional suppressive effects on the malignant phenotype when compared with the parental cells and vector controls. These cells showed decreased plating efficiency, elongated cell population doubling time, lower clonogenic fraction in soft agar, and, more significantly, inhibition of tumor formation in nude mice. This work suggested that *CuZnSOD* is a new tumor suppressor gene. Increased intracellular ROS levels were found in cells with high activity ratios of CuZnSOD:GPx. Change in the cellular redox status, especially change attributable to the accumulation of hydrogen peroxide or other hydroperoxides, is a possible reason to explain the suppression of tumor growth observed in CuZnSOD-overexpressing cells.

INTRODUCTION

ROS[3] are oxygen-containing molecules that have higher chemical reactivity than ground-state molecular oxygen. ROS include not only oxygen-centered radicals such as superoxide radical anion ($O_2^{\cdot-}$) and hydroxyl radical ($HO^{\cdot}$) but also molecules such as singlet oxygen ($^1O_2$) and hydrogen peroxide (H_2O_2). Currently, ROS are being implicated in the pathogenesis of a growing number of disease processes. Carcinogenesis (1–5), neurodegeneration (6), and aging (7) are all thought to have a ROS component in their pathogenesis.

Oxidative stress is the outcome of the imbalance between oxidant production and the cellular antioxidant capacity. The primary antioxidant enzymes that protect cells from oxidative damage include the SOD family, CAT, and the GPx family. Intracellular CuZnSOD and MnSOD catalyze the conversion of superoxide ($O_2^{\cdot-}$) to hydrogen peroxide (H_2O_2), which is further removed by CAT and GPx.

At least three isoforms have been found for SOD. In eukaryotes, MnSOD is a M_r 88,000 tetrameric protein that is localized primarily to the mitochondrial matrix (8). The purpose of MnSOD in this location is to remove $O_2^{\cdot-}$ generated by one-electron leakage from the electron transport chain. CuZnSOD is a M_r 32,000 dimeric protein that is localized in the cytoplasm (9). CuZnSOD in this location is thought to remove $O_2^{\cdot-}$ generated by endoplasmic reticulum and cytosolic as well as membrane oxidases. The third SOD isoform, extracellular SOD, is a M_r 135,000, tetrameric protein found in the extracellular space (10). Extracellular SOD may be important in removing membrane-related oxidase-generated $O_2^{\cdot-}$.

The relationship between the tumor cell phenotype and low CuZnSOD activity is poorly understood. Tumor cells treated with paraquat displayed increased SOD activity (probably CuZnSOD) and loss of the transformed phenotype (11). Further evidence suggested that CuZnSOD might be of importance in cancer cell invasion and metastasis (12, 13). Tumor cell invasion and metastasis are complex, multistep events that lead to the seeding of tumor cells at sites distant from the primary tumor. Muramatsu *et al.* (12) convincingly showed in *in vitro* studies that human tongue squamous carcinoma cells transfected with antisense *CuZnSOD* cDNA were more motile and invasive. A subsequent study using murine fibrosarcoma cells transfected with antisense *CuZnSOD* confirmed the earlier observations in an *in vitro* model of invasion by demonstrating the appearance of pulmonary metastases in mice from cells with decreased CuZnSOD expression (13).

Altered MnSOD and CuZnSOD levels have been found in many cancer cells. Overexpression of MnSOD has been shown to decrease the rate of tumor cell growth. Transfection of human *MnSOD* cDNA into MCF-7 human breast cancer cells (3), UACC-903 human melanoma cells (2), SCC-25 human oral squamous carcinoma cells (5), U118 human glioma cells (14), and DUI45 human prostate carcinoma cells (15) significantly suppressed their malignant phenotype. This suggested that MnSOD is a tumor suppressor gene in these cells and led to the hypothesis of the present study that overexpression of another essential antioxidant enzyme in the SOD family, CuZnSOD, will decrease the rate of tumor cell growth. Moreover, this work may provide additional insight into the mechanism of the tumor-suppressing effects of MnSOD. To test our hypothesis, we elevated CuZnSOD activity via stable transfection of *CuZnSOD* cDNA into the U118-9 glioma cell line. We demonstrated for the first time a tumor cell growth-suppressive effect of CuZnSOD overexpression.

MATERIALS AND METHODS

Cell Culture. The human glioma U118-9 cells were cloned from Wt U118 cells (14). The cells were grown in DMEM supplemented with 4.5 g/liter glucose and 10% fetal bovine serum (HyClone) at 37°C in a humidified atmosphere of 95% air and 5% CO_2. The cells were subcultured with 0.25% trypsin and 1% EDTA whenever the cultures reached confluence. Cells were used for analysis within 30 passages because it has been demonstrated that antioxidant enzyme levels do not change in tumor cells for up to 50 passages (16). Cells were regularly tested for *Mycoplasma* and used only if they were *Mycoplasma* free.

Vector Construction. Human *CuZnSOD* cDNA was originally isolated from the pEF-bos plasmid (kindly provided by Dr. Borchelt; Alzheimer's

Received 8/8/01; accepted 12/17/01.

The costs of publication of this article were defrayed in part by the payment of page charges. This article must therefore be hereby marked *advertisement* in accordance with 18 U.S.C. Section 1734 solely to indicate this fact.

[1] Supported by NIH Grant CA 66081 (to L. W. O.).

[2] To whom requests for reprints should be addressed. Phone: (319) 335-8015; Fax: (319) 335-8039; E-mail: larry-oberley@uiowa.edu.

[3] The abbreviations used are: ROS, reactive oxygen species; CAT, catalase; CuZnSOD, copper zinc superoxide dismutase; DCFH-DA, 2′,7′-dichlorodihydrofluorescein diacetate; GPx, glutathione peroxidase; MnSOD, manganese superoxide dismutase; RT-PCR, reverse transcription-PCR; SOD, superoxide dismutase; NBT, nitroblue tetrazolium; Wt, wild type; DCF, dichlorofluorescein; TEMED, *N*,*N*,*N*′,*N*′-tetramethylethylenediamine.

Disease Research Center, Baltimore, MD) and then recombined into the pBluescript plasmid. Finally, *CuZnSOD* cDNA was inserted into the pcDNA3 mammalian expression vector (Invitrogen, Carlsbad, CA) between the *Kpn*I and *Eco*RV sites, driven by a cytomegalovirus promoter. The vector also includes a *Neo* resistance gene driven by the SV40 promoter for clone selection.

Transfection. U118-9 cells were stably transfected with pcDNA3 plasmid containing sense human *CuZnSOD* cDNA or containing no *CuZnSOD* insert by using the LipofectAMINE (Life Technologies, Inc., Gaithersburg, MD) method. The G418-resistant colonies were isolated by the ring cloning method and maintained in medium supplemented with 400 μg/ml G418 (Life Technologies, Inc.). Five days before an analysis, cells were placed into complete medium without antibiotic supplement.

Protein Sample Preparation. The procedures for protein sample preparation were performed on ice. The cells were washed twice with PBS, harvested by scraping, and sonicated in 50 mM phosphate buffer (pH 7.8) on ice with four bursts of 30 s each using a Vibra Cell Sonicator (Sonics and Materials Inc., Danbury, CT) with a cup horn at full power. Total protein concentrations were determined by the Bio-Rad (Hercules, CA) Bradford protein assay kit using lyophilized bovine plasma γ-globulin as standard.

Western Blot Analysis. A total of 150 μg of denatured protein was separated by 12.5% SDS-PAGE, electrotransferred onto a nitrocellulose membrane, and then probed with antiserum to human CuZnSOD (diluted 1:1000). Polyclonal rabbit antibodies to human CuZnSOD have been prepared and characterized in our laboratory (17). The CuZnSOD-immunoreactive bands were detected by an enhanced chemiluminescence kit (Amersham, Arlington Heights, IL). The bands were visualized and quantified with a computerized digital imaging system using AlphaImager 2000 software (Alpha Innotech, San Leandro, CA). The integrated density value was obtained by integrating all of the pixel values in the area of one band after correction for background.

Northern Blot Analysis. Total RNA was extracted from 80% confluent cells using a RNAzol kit (Tel-test, Inc., Friendswood, TX). Northern blot analysis was performed as described previously (18). The membrane was hybridized with a 500-bp digoxigenin-labeled human *CuZnSOD* cDNA.

RT-PCR. Vector-specific oligonucleotide primers for human *CuZnSOD* cDNA were synthesized at the DNA Core Facility at the University of Iowa according to the DNA sequence of the recombination product of pcDNA3 and human *CuZnSOD* cDNA. The sequences were as follows: sense, 5′-TCGAG-GTCGACAAGCATGGC-3′; and antisense, 5′-CTGCAGAATTCGATAT-CAAG-3′. The PCR product was approximately 500-bp long. These primers were designed so that only one band of exogenous *CuZnSOD* gene was seen in *CuZnSOD*-transfected clones because part of the sequences of the primers was from the pcDNA3 vector. A similar method was used previously to specifically detect mRNA from a transfected *MnSOD* cDNA (19). RT-PCR was performed as described previously (4).

Antioxidant Enzyme Activity Assays. SOD activity was measured by the modified NBT method described by Spitz and Oberley (20) and a modified native activity gel assay as described by Beauchamp and Fridovich (21). MnSOD activity was quantified in the presence of 5 mM NaCN, which inhibits only the CuZnSOD activity. CuZnSOD activity was determined by subtracting MnSOD activity from total SOD activity. One unit of activity was defined as the concentration of SOD that inhibited the NBT reduction rate to half of the maximum. Errors in CuZnSOD activity were determined by propagation of error theory. CAT activity was measured by directly monitoring the decomposition of H_2O_2 as described by Claiborne (22). GPx activity was measured by an indirect assay that monitors the disappearance of NADPH as described by Gunzler and Flohe (23).

Intracellular ROS Measurement. The level of intracellular ROS was determined by measuring the oxidation of DCFH-DA (Molecular Probes Inc., Eugene, OR; Ref. 24). An oxidation-insensitive fluorescent probe, 5-(and -6)-carboxy-2′,7′-dihydrodichlorofluorescein diacetate [carboxy(1)-DCFDA, C369; Molecular Probes Inc.], was used as a control for esterase activity. DCFH-DA is a nonpolar and nonfluorescent compound that can permeate cells freely. When inside cells, it is hydrolyzed by esterase to form the polar and nonfluorescent dichlorodihydrofluorescein. Upon interaction of dichlorodihydrofluorescein with ROS, it gives rise to DCF that yields fluorescence. Cells (200,000) from each clone were seeded 24 h before measurement in a 24-well dish. On the day of assay, the cells were washed twice with serum-free medium and then incubated with 0.5 ml of 30 μM DCFH-DA solution for 90 min at 37°C. After the incubation, the cells were washed twice with PBS buffer and then lysed in 0.5 ml of 0.5% SDS solution. Finally, the intensity of the 485/530 nm fluorescence corresponding to the levels of intracellular ROS in the lysates was recorded with a microplate reader (Bio-Tec Instruments, Winooski, VT) using FL500 software. The relative fluorescence was calculated by the following equation:

$$\text{Relative fluorescence}/10^4 \text{ cells} = \frac{(\text{Reading of the cells treated with DCFH-DA} - \text{reading of blank})}{\text{Cell number}} \quad (1)$$

where the blank contained cells in medium without DCFH-DA.

Plating Efficiency. Cells (500–1000) were plated in 60-mm culture dishes, incubated for 14 days to allow colony formation, and then fixed and stained with 0.1% crystal violet. The colonies containing ≥50 cells were scored. The plating efficiency (*PE*) was calculated as follows:

$$PE = (\text{Colonies formed/Cells seeded}) \times 100\% \quad (2)$$

Growth Curve. Cells (20,000) of each clone were plated in a 24-well dish. The growth rate of cells was determined by counting the number of cells with a hemocytometer as a function of time. Cell population doubling time (*Td*) was calculated from the growth rate during exponential growth by the following formula:

$$Td = 0.693t/ln(N_t/N_0) \quad (3)$$

where t is time in days, N_t is the cell number at time t, and N_0 is the cell number at the initial time.

Soft Agar Clonogenic Assay. Cells (1000–3000) were suspended in 3 ml of culture media with 0.3% agar. This cell suspension was overlaid onto 3 ml of presolidified 0.5% agar in 60-mm dishes. After 4 weeks of incubation, the number of colonies >0.1 mm in diameter was counted. The cell clonogenic fraction was calculated using the following equation:

$$\text{Clonogenic fraction} = (\text{Colonies counted/Number of cells seeded}) \times 100\% \quad (4)$$

Tumorigenicity in Nude Mice. Female nude (*nu/nu*) mice (4–5 weeks old; Harlan Sprague Dawley, Madison, WI) were used. Cells (2,000,000; 0.1 ml) were injected s.c. into the back of the neck of each nude mouse. Four nude mice were used for each group. When the tumor was palpable, it was measured by a vernier caliper once every 7 days. Tumor volume (*TV*) was calculated as follows:

$$TV\ (\text{mm}^3) = (L \times W^2)/2 \quad (5)$$

where L is the longest dimension of the tumor (in mm), and W is the shortest dimension of the tumor (in mm; Refs. 4 and 14).

Statistics. The statistics were done by SYSTAT, a computer statistical package. ANOVA-Tukey was used for the analysis. Regression and correlation analysis were used to determine the relationship between the growth characteristics and CuZnSOD activity. All Western and Northern blots were run at least twice to show reproducibility.

RESULTS

Expression of CuZnSOD in Transfectants. To overexpress human sense *CuZnSOD* cDNA in U118-9 cells, the pcDNA3/Neo/hSOD1 expression vector was constructed. Three vectors were used to make the final plasmid constructs. Human *CuZnSOD* cDNA was isolated from the pEF-bos vector, recombined with the pBluescript vector at the *Sal*I site, and inserted into the pcDNA3 expression vector between the *Kpn*I and *Eco*RV sites.

The transfected clones resistant to G418 were screened using Western blotting. Four clones with higher levels of CuZnSOD protein were selected for further study. They were designated as C-3, C-5, C43, and C51 according to their original clone number. Wt is U118-9 parental

cells, and Neo is a clone transfected with the pcDNA3 vector plasmid without *CuZnSOD* cDNA.

The expression of CuZnSOD was verified by Western blotting, Northern blotting, and RT-PCR. The expression of CuZnSOD protein was measured by Western blot analysis as shown in Fig. 1*A*. The results showed increased CuZnSOD-immunoreactive protein in the four CuZnSOD transfectants, compared with that seen in parental and Neo control cells. Computerized analysis of densitometric scanning demonstrated that the amount of immunoreactive protein was increased over the parent and Neo control cells by 1.5-, 2-, 3.5-, and 2.5-fold in clones C-3, C-5, C43, and C51, respectively.

To determine whether the increased CuZnSOD protein resulted from the expression of the exogenous cDNA, Northern blot analysis was performed using a digoxigenin-labeled *CuZnSOD* cDNA probe. For human CuZnSOD, there are two known endogenous mRNA bands (about 0.7 and 0.9 kb, respectively). The results showed that an increased intensity at about 0.9 kb appeared in all four transfectants (Fig. 1*B*). The similar position between the exogenous and endogenous CuZnSOD mRNA at 900 bp is reasonable because: (*a*) the coding region for *CuZnSOD* cDNA is about only 500 bp in length; (*b*) the size of the new bands correspond to that of the *CuZnSOD* cDNA 500-bp fragment plus a signal sequence (about 350 bp) from the pcDNA3 vector; and (*c*) the mRNA level showed a similar pattern with the protein expression level. The insertion of exogenous *CuZnSOD* cDNA was further confirmed by RT-PCR (Fig. 1*C*). RT-PCR results indicated that the increased CuZnSOD mRNA expression

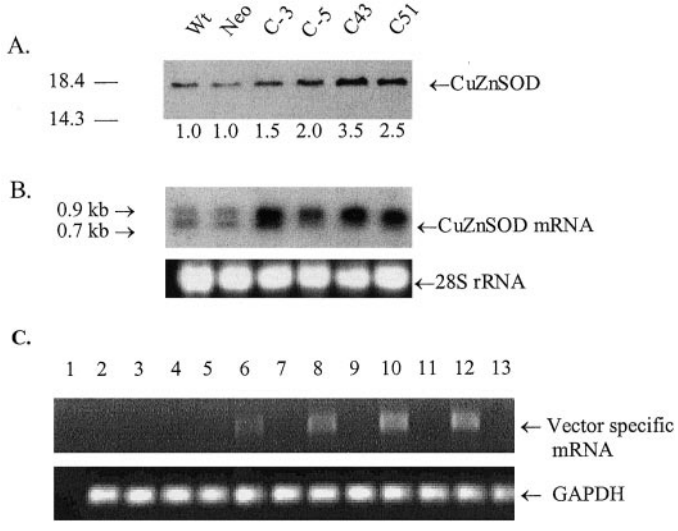

Fig. 1. *CuZnSOD*-transfected clones showed increased CuZnSOD expression at the mRNA and protein levels. *A*, the protein level of CuZnSOD was analyzed by Western immunoblotting. A total of 50 μg protein/lane was used. The *top panel* shows a representative blot indicating increased CuZnSOD protein expression in four transfected cell lines (C-3, C-5, C43, and C51). The Neo clone (transfected with vector only) had an expression level similar to that of Wt. The *number under* each lane shows the densitometric analysis. The *numbers* to the *left* indicate positions of molecular weight markers. *B*, expression from the transfected plasmid was examined by Northern blot analysis. Twenty μg of total RNA from each sample were electrophoresed and then transferred to a nylon membrane. The blot was hybridized with a digoxigenin-labeled *CuZnSOD* cDNA probe. Ethidium bromide staining of 28S (~5 kb) rRNA was used as a loading control. The stable transfectants displayed considerably more CuZnSOD mRNA than did parental and Neo controls. *C*, detection of exogenous vector-derived CuZnSOD mRNA by RT-PCR. cDNA synthesis was carried out from 5 μg of total RNA in a 30-μl reaction solution. Two μl of cDNA (dilution of reverse transcription products at 1:100) were amplified in a 20-μl PCR mixture for 30 cycles. Fifteen μl of PCR products were separated in a 1.2% agarose gel with ethidium bromide staining and compared with 1-kb DNA ladders. The specific exogenous bands (0.5 kb) were found only in CuZnSOD transfectants (19). *Lane 1*, PCR reaction without DNA template as negative control (the remaining negative controls were run with template that had not been reverse transcribed); *Lane 2*, Wt; *Lane 4*, Neo; *Lane 6*, C-3; *Lane 8*, C-5; *Lane 10*, C43; *Lane 12*, C51. The RNA samples were used directly as templates for PCR reaction. *Lane 3, 5, 7, 9, 11*, and *13* were the negative controls for *lane 2, 4, 6, 8, 10*, and *12*, respectively.

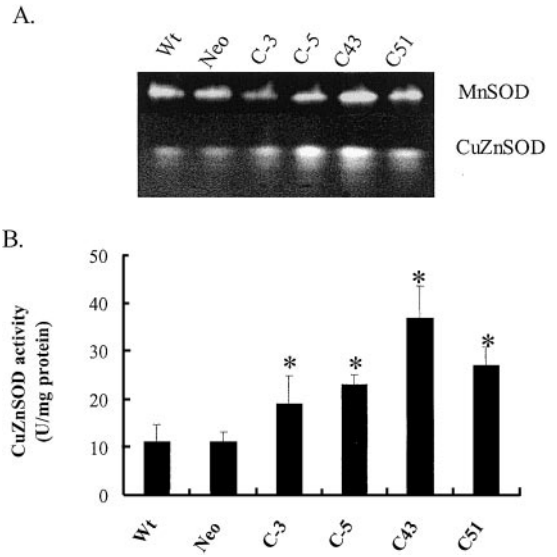

Fig. 2. CuZnSOD activity was increased in the transfected clones. *A*, activity gel showed bands with significantly increased intensity in CuZnSOD transfectants. Proteins (100 μg/lane) were separated on a native polyacrylamide gel. The gel was then stained by incubation with 2.43 mM NBT, 28 mM riboflavin, and 28 mM TEMED for 20 min in the dark. After exposing the gel to a fluorescent light, the achromatic bands corresponding to SOD appeared on a dark blue background. A representative gel is shown. *B*, CuZnSOD activity was calculated by subtracting MnSOD activity from total SOD activity. Total SOD activity and MnSOD activity were measured by the competition reaction between SOD and NBT. One unit of SOD activity was defined as the concentration of SOD that reduces the NBT reaction to one-half of the maximum. Mean ± SE; $n \geq 5$ (five independent samples); *, $P \leq 0.05$.

came largely from the expression of exogenous CuZnSOD mRNA rather than increased expression of the endogenous *CuZnSOD* gene. Because we used vector-specific primers, a 500-bp band was seen only in the four transfected clones and not in parental and Neo cells. Among the four transfectants, C43 had the highest mRNA expression, which is consistent with the results from Western blotting and Northern blotting. Clone C-3 demonstrated the lowest expression among the transfectants, whereas it showed a very high expression with Northern blotting. This may be due to increased expression of the endogenous gene in clone C-3 as well as that from the exogenous cDNA. This is consistent with the increased level of the 0.7-kb transcript seen in this clone only. These results demonstrated that the foreign *CuZnSOD* cDNA has been stably transfected into the genome and caused increased expression of CuZnSOD at the mRNA and protein levels.

Increases in CuZnSOD Enzymatic Activity. CuZnSOD enzymatic activity was measured by native gel electrophoresis analysis (Fig. 2*A*) and SOD activity spectrophotometric assay (Fig. 2*B*; Table 1). Native electrophoresis showed that all four transfectants had greater CuZnSOD activities than the parental and Neo controls. Clone C43 had the highest enzyme activity level and also expressed the highest level of CuZnSOD mRNA and protein. Compared with the parental and Neo control cells (11 units/mg protein), clones C-3, C-5, and C51 had a 1.5–2.6-fold increase (16–28 units/mg protein) in activity, whereas C43 had a 3.5-fold increase (38 units/mg protein). The increased amount of CuZnSOD activity was parallel to that of CuZnSOD mRNA and protein.

The activities of MnSOD, CAT, and GPx were also examined (Table 1). All *CuZnSOD* transfectants (except clone C-3) had increased MnSOD enzyme activity when compared with parental and Neo cells. When correlation analysis was performed on MnSOD activity *versus* CuZnSOD activity, a statistically significant correlation was observed ($r = 0.90$; $P = 0.02$). However, the changes in MnSOD were small (a maximum 40% increase) compared with CuZnSOD activity. Two clones had decreased CAT activity, whereas

Table 1 *Antioxidant enzyme activities in the parental, Neo control, and CuZnSOD-transfected cells*

Cells	CuZnSOD[a] (units/mg protein)	MnSOD[a] (units/mg protein)	CAT[b] (k/g protein)	GPx[a] (units/mg protein)	CuZnSOD:GPx ratio
Wt	11 ± 4	56 ± 2	341 ± 9	11 ± 1	1.0
Neo	11 ± 2	54 ± 1	330 ± 7	8 ± 1	1.6
C-3	19 ± 6[c]	52 ± 3	435 ± 8[c]	8 ± 1	2.4
C-5	23 ± 2[c]	65 ± 1[c]	298 ± 5	17 ± 4[c]	1.4
C43	37 ± 7[c]	78 ± 4[c]	197 ± 5[c]	11 ± 1	3.5
C51	27 ± 4[c]	62 ± 3[c]	320 ± 5	15 ± 3[c]	1.8

[a] Results are expressed as the mean ± SE from at least five independent samples.
[b] Results are expressed as the mean ± SE from three independent samples. k units are catalytic rate constant units as defined in Ref. 22.
[c] $P < 0.01$ compared to Wt control cells.

the other two did not. Only clones C-5 and C51 had increased GPx activities compared with the controls. Although clone C43 had the highest CuZnSOD and MnSOD activity, it had the lowest CAT activity of all clones. Finally, the ratios of CuZnSOD and GPx activities were calculated and listed in Table 1 for the reasons discussed below. Clone C-3 and clone C43 had the highest ratios of all the transfectants.

Effects of CuZnSOD Overexpression on U118-9 Cell Growth *in Vitro*. Tumor cell growth characteristics were used to evaluate the effect of the overexpression of CuZnSOD in cell culture. The growth curve, cell population time, plating efficiency, and anchorage independence were therefore examined.

Growth curves were assessed by seeding cells in 24-well tissue culture plates at 2×10^4 cells/well and then counting the cell number every other day. Although the four CuZnSOD transfectants displayed different growth rates, all of them grew more slowly than the parental and Neo cell lines (Fig. 3*A*). C-3 and C43 had the lowest growth rates. When the cell numbers at day 11 were compared, clone C43 was the lowest with approximately 42% inhibition of cell growth.

Cell population doubling times were calculated from cell growth curves (Fig. 3*B*). Compared with Wt and Neo, which had doubling times of 43.5 and 50.4 h, respectively, CuZnSOD-transfected cells displayed variable increases in doubling times, ranging from 51.4 to 76.5 h. Because many of the antioxidant enzymes changed after CuZnSOD transfection, we performed correlation analysis to determine whether doubling time correlated with CuZnSOD activity. As shown in Table 2, correlation with CuZnSOD activity alone was low and was not statistically significant ($r = 0.56$; $P < 0.50$). For this reason, we correlated cell doubling time *versus* all of the biologically relevant antioxidant enzyme activities or their ratios that we could think of. The results are shown in Table 2. The only statistically significant correlations are *versus* the CuZnSOD:GPx ratios and the CuZnSOD:MnSOD ratios. We think the CuZnSOD:GPx ratio is the most significant for the following reasons: (*a*) it had the highest correlation; (*b*) both proteins are in the same subcellular compartments (cytoplasm and nucleus); and (*c*) others have also stressed the coupling of these two proteins (25, 26). These results suggested that the decreased growth rate was strongly related to the high enzyme activity ratio of CuZnSOD:GPx, and this is the ratio used for the other correlations performed. As shown in Fig. 3*C*, doubling time correlated very strongly with the CuZnSOD:GPx activity ratio ($r = 0.92$; $P = 0.02$). Clones 3 and 43, which had the higher CuZnSOD:GPx ratio, grew much more slowly.

Plating efficiency is a measure of clonogenic ability of cells. Cancer and transformed cells in general have higher plating efficiencies than normal cells. This assay was performed by seeding 500 cells in a 60-mm culture dish and counting the number of colonies formed in 2 weeks. The plating efficiencies were significantly decreased in the CuZnSOD-overexpressing cells compared with parent and Neo cells, with the exception of C-5 (Fig. 4*A*). The possible explanation is that C-5 has an increased endogenous GPx activity. In support of this, when plating efficiency was plotted against the CuZnSOD:GPx ratio (Fig. 4*B*) and a correlation analysis was performed, a highly significant negative correlation was found ($r = -0.94$; $P < 0.05$).

The soft agar assay illustrates anchorage-independent growth. For this assay, a single cell suspension was seeded in 0.3% agar, and colonies were allowed to form for 4 weeks. The results are shown in Fig. 5*A*. The CuZnSOD-overexpressing clones grew poorly in soft

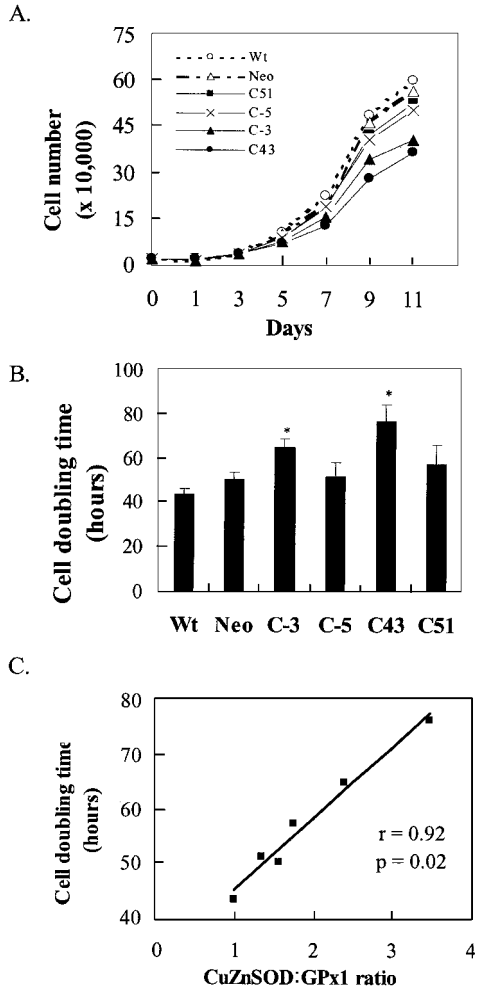

Fig. 3. CuZnSOD overexpression inhibited cell growth *in vitro*. *A*, growth curve. Cells (20,000) were seeded in 24-well dishes. Cell numbers were counted on days 1, 3, 5, 7, 9, and 11. The data in the graph must be multiplied by 10,000 to obtain the correct cell number. The results show that overexpression of CuZnSOD inhibited tumor cell growth *in vitro*. Means are shown for three experiments. *B*, cell population doubling time. Cell population doubling time was calculated from the cell growth curve during the exponential growth phase (day 3 to day 9) according to the equation $Td = 0.693t/\ln(N_t/N_0)$, where t is time (in h), N_t is the cell number at time t, and N_0 is the cell number at initial time. Mean ± SE; $n = 3$; *, $P < 0.05$. CuZnSOD overexpression led to increased doubling times. *C*, correlation analysis of doubling times *versus* CuZnSOD:GPx activity ratio. $P < 0.05$.

agar compared with parental cells, which gave rise to 4.16% colony formation efficiency. Clone C-5 had higher colony formation efficiency in soft agar than the other three CuZnSOD-overexpressing clones. This is consistent with its higher plating efficiency on plastic as compared with the other clones. Linear regression analysis of the relationship of colony formation efficiency and CuZnSOD:GPx ratio (Fig. 5*B*) gave a correlation coefficient of $r = -0.79$ ($P < 0.05$).

Increases in Steady-state Levels of Intracellular ROS. The intracellular ROS levels were measured by the dichlorofluorescein fluorescence method (Fig. 6*A*). This assay measures oxidation by various ROS, including those derived from hydrogen peroxide. The intracellular ROS levels in CuZnSOD-overexpressing clones were dramatically increased to about 3–5-fold greater than those of parental and Neo cells. The oxidation-insensitive fluorescence probe C369 was used as control and showed no difference between parental and C43 cells (Fig. 6*B*). The levels of intracellular ROS were correlated to the ratios of SOD:GPx activity. When dichlorofluorescein fluorescence was plotted against the activity ratio of CuZnSOD:GPx (Fig. 6*C*), a significant positive correlation was found ($r = 0.83$; $P < 0.05$). Population doubling time also showed a highly significant correlation with dichlorofluorescein fluorescence (Fig. 6*D*; $r = 0.91$; $P < 0.05$).

Table 2 *Correlation analysis of cell doubling times versus antioxidant enzyme activities*

Cell doubling time *vs.* different factors	*r* (correlation coefficient)	*P*
CuZnSOD activity	0.56	<0.50
MnSOD activity	0.61	<0.50
Total SOD activity	0.74	<0.20
CAT activity	0.37	<0.50
GPx activity	0.23	>0.50
MnSOD:GPx ratio	0.65	<0.50
Total SOD:GPx ratio	0.81	<0.20
Total SOD:CAT ratio	0.71	<0.20
Total SOD:(GPx + CAT) ratio	0.72	<0.20
CuZnSOD:GPx ratio	0.92	0.02[a]
MnSOD:CAT ratio	0.65	<0.20
CuZnSOD:CAT ratio	0.80	<0.10
CuZnSOD:MnSOD ratio	0.84	0.04[a]
CuZnSOD:(GPx + CAT) ratio	0.80	<0.10
MnSOD:(GPx + CAT) ratio	0.66	<0.20

[a] $P < 0.05$ compared to Wt control cells.

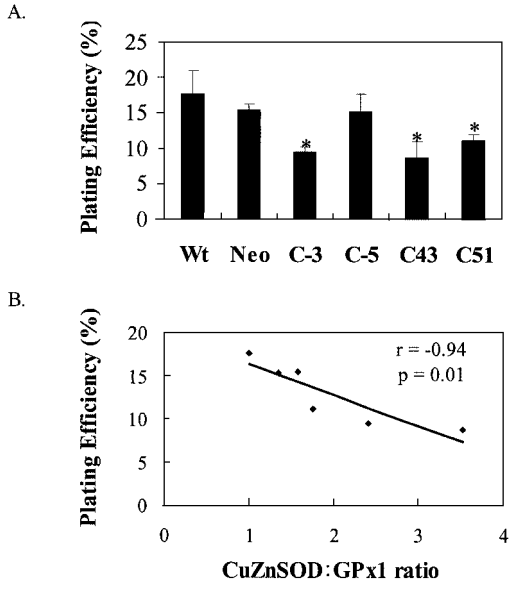

Fig. 4. CuZnSOD overexpression decreased cell plating efficiency. *A*, cell plating efficiency. Cells (500) were seeded in 60-mm dishes and grown for 2 weeks. Colonies with >50 cells were counted. Mean ± SE; $n = 3$; ∗, $P < 0.05$. *B*, correlation analysis of plating efficiency *versus* CuZnSOD:GPx activity ratio. $P < 0.05$.

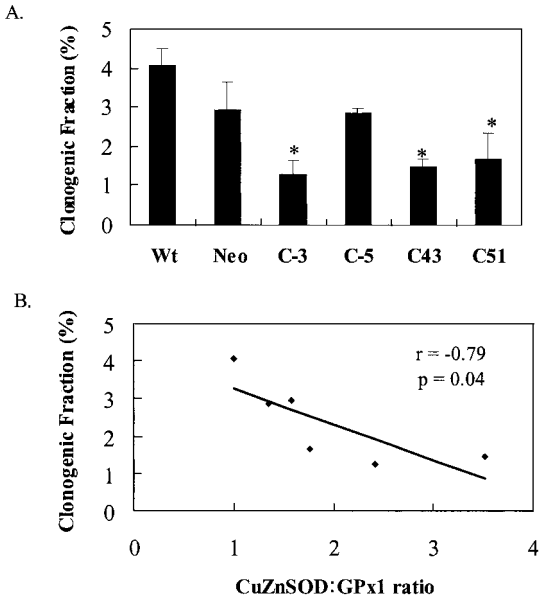

Fig. 5. CuZnSOD overexpression decreased cell anchorage-independent growth. *A*, the overexpression of CuZnSOD significantly suppressed the cell clonogenic ability in soft agar. Cells (1000–3000) of each clone were plated in 60-mm dishes with 3 ml of culture media containing 0.3% agar solution. After 4 weeks of incubation, the number of colonies >0.1 mm in diameter was counted. Mean ± SE; $n = 3$; ∗, $P < 0.05$. *B*, correlation analysis of clonogenic fraction in soft agar *versus* CuZnSOD:GPx activity ratio. $P < 0.05$.

Effect of CuZnSOD on U18-9 Cell Growth *in Vivo*. Tumorigenicity was determined by transplanting tumor cells s.c. in the back of the neck of nude mice. This experiment was designed to test the role of CuZnSOD in the suppression of tumor cell growth *in vivo*. The results of the tumor growth experiment are shown in Fig. 7 and Table 3. Tumor growth was dramatically inhibited by CuZnSOD overexpression. The CuZnSOD-overexpressing cell line formed tumors that grew much slower than those of the parental or Neo cell line. C-3 and C43 had the slowest growth rate (Fig. 7). These results demonstrated that the low growth rate was strongly related to a high enzyme activity ratio of CuZnSOD:GPx. Clones C-3 and C43 with the higher CuZnSOD:GPx ratios grew much more slowly. We could neither measure doubling times in this experiment nor perform correlation analysis because not all of the tumors showed exponential growth. These results show convincingly that CuZnSOD overexpression suppresses tumor cell growth. Tumor incidence showed a similar picture (Table 3). Parental and Neo cells had a high tumor incidence, which was suppressed by CuZnSOD overexpression.

DISCUSSION

CuZnSOD and MnSOD are essential antioxidant enzymes that catalyze the conversion of superoxide radical ($O_2^{\cdot-}$) to hydrogen peroxide (H_2O_2), which is further converted to harmless water by CAT and GPx. In the past years, many scientists have focused on the study of MnSOD. Overexpression of MnSOD has been shown to decrease the rate of tumor cell growth. Mechanisms by which this antioxidant enzyme suppresses the malignant phenotype are currently unclear. The relationship between the tumor cell phenotype and low CuZnSOD activity has been little studied. We expected to see that overexpression of CuZnSOD might reverse at least part of the cancer cell phenotype. The importance of CuZnSOD in cancer has been shown recently by transfecting antisense *CuZnSOD* cDNA and demonstrating increased metastasis (13). The current work demonstrates that overexpression of CuZnSOD also inhibits cancer cell growth.

Three criteria for measuring cell growth are generally recom-

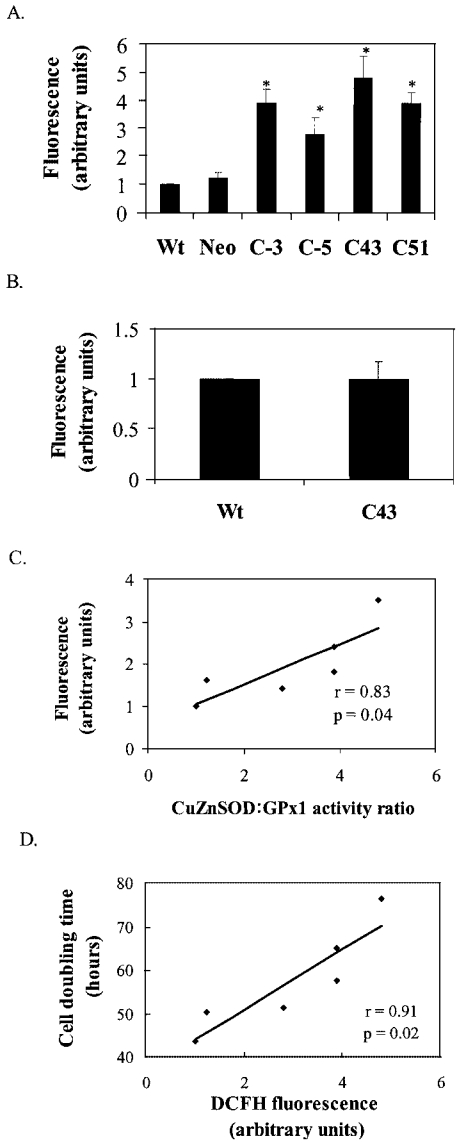

Fig. 6. Intracellular ROS were increased in CuZnSOD-overexpressing clones. *A*, measurement of intracellular ROS in different samples. Cells were stained with the oxidation-sensitive fluorescence probe DCFH-DA. The intensity of the 480/530 nm fluorescence of DCFH-DA, corresponding to the levels of intracellular ROS in the lysates, was recorded with a microplate reader (Bio-Tek Instruments, Inc.) using FL500 software. Mean ± SE; $n \geq 3$; *, $P \leq 0.05$. CuZnSOD transfectants had significantly higher levels of dichlorofluorescein fluorescence compared with the control. *B*, measurement of ROS generation using the oxidation-insensitive probe C369. The oxidation-insensitive fluorescence probe C369 was used as control for dye uptake, ester cleavage, and efflux. Mean ± SE; $n \geq 3$. *C*, correlation analysis of intracellular ROS *versus* CuZnSOD:GPx activity ratio. $P < 0.05$. *D*, correlation analysis of cell population doubling time *versus* intracellular ROS levels. $P < 0.05$.

mended to determine the characteristics of the tumor cell malignant phenotype: (*a*) *in vitro* cell growth measured by growth rate and clonogenic ability; (*b*) *in vitro* growth in soft agar; and (*c*) *in vivo* tumor formation in nude mice. It is generally believed that *in vitro* tumor cells have the ability to grow faster, to form more colonies, and to grow better in soft agar than normal cells. *In vivo*, malignant cells can form tumors in immunodeficient mice. We evaluated our CuZnSOD-overexpressing cells by these three criteria for tumor cell malignant phenotype. Our results demonstrated that increased CuZnSOD activity in human malignant glioma U118-9 cells inhibited cell growth rate with elongated tumor doubling times in most of the CuZnSOD-overexpressing clones. These CuZnSOD-overexpressing cells also showed lower plating efficiency, lower clonogenic fraction in soft agar, and delayed onset or no tumor formation in nude mice as compared with their counterparts, the nontransfected parental cells and vector-transfected control cells. Our results suggested that CuZnSOD is a tumor suppressor in human glioma cancer. One might argue that the results are due to MnSOD rather than CuZnSOD, given the fact that three of the four clones had higher MnSOD activity and that MnSOD is a known tumor suppressor. However, the measured changes in MnSOD were small (40% maximum) compared with the changes in CuZnSOD. Previous work has shown that much larger changes in MnSOD (about 5-fold) were necessary to cause tumor suppression (2). Moreover, as shown in Table 2, the correlations that involved MnSOD were not statistically significant, with the exception of doubling time *versus* the CuZnSOD:MnSOD ratio, which also involved CuZnSOD. Thus, the measured changes appear to be due mainly to CuZnSOD and only to a smaller extent to MnSOD.

It is not surprising that our results show changes in endogenous GPx and CAT activities in CuZnSOD transfectants (Table 1). Organisms have evolved antioxidant defenses to protect against ROS, predominant among which is the enzymatic antioxidant pathway. This pathway consists of essentially two steps: (*a*) first, the dismutation of superoxide into hydrogen peroxide by SODs; and (*b*) second, the conversion of hydrogen peroxide to water that is catalyzed by GPx and/or CAT. Theoretically, the balance between the first and second step antioxidant enzymes is critical (27): on the one hand, too little SOD relative to GPx and/or CAT could result in an accumulation of superoxide radicals that are toxic to macromolecules; on the other hand, too much SOD relative to GPx and/or CAT could lead to increased hydrogen peroxide, which can be converted to $^{\bullet}OH$ in the Fenton reaction (28). $^{\bullet}OH$ is a very reactive species that is responsible for much oxidative damage to the cell.

The intracellular ROS levels as measured by DCFH-DA fluorescence (Fig. 6) suggested that CuZnSOD overexpression leads to accumulation of H_2O_2, which causes high fluorescence intensity of DCFH-DA. GPx, can remove H_2O_2, so there was lower fluorescence intensity in both C-5 and C51 clones with increased endogenous GPx activities. In mammalian cells, overexpression of SOD in cells bearing

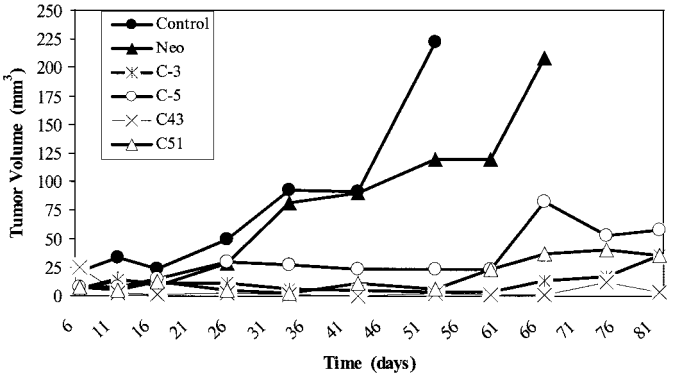

Fig. 7. CuZnSOD overexpression inhibited tumor growth *in vivo*. Tumorigenicity was assessed in female nude mice. Cells (2,000,000) were transplanted s.c. in the back of the neck of female nude mice. Tumor length (*L*) and width (*W*) were measured once a week by vernier caliper. Tumor volume (*TV*) was calculated by the formula $TV\ (mm^3) = (L \times W^2)/2$. There were four mice in each group, and all mice were included in the calculations of tumor volume.

Table 3 *Tumor incidence in nude mice*[a]

Cell lines	Wt	Neo	C-3	C-5	C43	C51
Incidence (%)	100 (4/4)	100 (4/4)	100 (4/4)	100 (4/4)	25 (1/4)	75 (3/4)

[a] Tumor incidence = (the number of mice with tumor/the number of total mice) × 100%.

extra copies of the SOD gene produced a higher sensitivity to ROS. In these cases, it has been postulated that SOD overexpression would lead to accumulation of H_2O_2 (29, 30). Overexpression of CuZnSOD can cause different responses in different systems. A compensatory increase in GPx1 occurred as a consequence of the introduction of the CuZnSOD expression vector into L cells, neuroblastoma cells, and primary mouse cells (31, 32). Transfection of a *CuZnSOD* expression vector into 3T3 murine fibroblasts resulted in two classes of transfectants, which were characterized by the presence or absence of an increase in endogenous GPx. In the transfectants with the absence of an increased endogenous GPx, hydrogen peroxide was accumulated intracellularly (25). Subsequent transfection of *CAT* or *GPx1* (29, 26) into those CuZnSOD-overexpressing cells compensated for the sensitizing effect of CuZnSOD. In our experiments, hydrogen peroxide (or other peroxides) produced by elevated CuZnSOD activities was further removed by increased endogenous GPx in clones C-5 and C51. On the other hand, hydrogen peroxide was increased (probably due to low GPx), resulting in higher dichlorofluorescein fluorescence in clones C-3 and C43.

Thus, our results seem to be due to increased levels of hydrogen peroxide. This is a controversial area because many scientists have claimed that hydrogen peroxide levels do not increase after SOD overexpression. We have argued that hydrogen peroxide levels do increase based on three observations: (*a*) CAT or GPx usually increases after SOD transfection; (*b*) dichlorofluorescein fluorescence increases after SOD transfection; and (*c*) overexpression of either GPx (33) or CAT (34) inhibits the tumor-suppressive effect of MnSOD transfection. Why does hydrogen peroxide increase? We are working on a mathematical model that shows that removal of superoxide by SOD causes superoxide-producing reactions to make more product (for example, coenzyme Q making more superoxide) because of the law of mass action. This makes more superoxide that can be dismuted by SOD to make more hydrogen peroxide. This model will be published in the future.

In the growth rate results, we also found that C-5 and C51 clones grew faster than the C-3 and C43 clones. This might result from the fact that the C-5 and C51 clones had lower intracellular ROS levels than the C-3 and C43 clones. It suggests that intracellular ROS at certain levels can affect cell growth. We showed previously that ras-mediated effects on cell growth are associated with increased O_2^- production and can be blocked by SODs (35, 36). A number of other normal cells and tumors can produce H_2O_2 and O_2^- *in vitro* either in response to various stimuli or constitutively (29). Experiments have also indicated that low concentrations of O_2^- and H_2O_2 (10 nM to 1 μM) were effective in stimulating the *in vitro* growth of hamster and rat fibroblasts when added to the culture medium (37, 38). Using xanthine/xanthine oxidase to generate ROS, Rao and Berk (39) demonstrated that H_2O_2 could stimulate rat vascular smooth muscle cell growth. This evidence suggests that H_2O_2 and O_2^- can stimulate growth and growth responses in a variety of cultured mammalian cell types when produced endogenously or added exogenously.

In summary, the relationship between increased CuZnSOD expression and the malignant phenotype has been studied in human glioma cells. Our results show that elevated CuZnSOD activity can reverse at least part of the malignant phenotype of U118-9 cells, suggesting that CuZnSOD may be a new tumor suppressor. Furthermore, H_2O_2 or other hydroperoxides may play a role in glioma tumor suppression by CuZnSOD overexpression. However, it was found that the ratio of CuZnSOD:GPx activity was important in cancer growth suppression. Therefore it is still unclear whether CuZnSOD by itself is a tumor suppressor; this is clearly different than the situation in MnSOD overexpression, where high correlations of various growth parameters have been found with MnSOD alone. Further work with double transfections of *CuZnSOD* and *CAT* or *GPx* will be necessary to clarify this issue of whether *CuZnSOD* is truly a tumor suppressor.

REFERENCES

1. Oberley, L. W., and Buettner, G. R. Role of superoxide dismutase in cancer: a review. Cancer Res., *39:* 1141–1149, 1979.
2. Church, S. L., Grant, J. W., Ridnour, L. A., Oberley, L. W., Swanson, P. E., Meltzer, P. S., and Trent, J. M. Increased manganese superoxide dismutase expression suppresses the malignant phenotype of human melanoma cells. Proc. Natl. Acad. Sci. USA, *90:* 3113–3117, 1993.
3. Zhang, H. J., Yan, T., Oberley, T. D., and Oberley, L. W. Comparison of effects of two polymorphic variants of manganese superoxide dismutase on human breast MCF-7 cancer cell phenotype. Cancer Res., *59:* 6276–6283, 1999.
4. Zhong, W., Oberley, L. W., Oberley, T. D., Yan, T., Domann, F. E., and St. Clair, D. K. Inhibition of cell growth and sensitization to oxidative damage by overexpression of manganese superoxide dismutase in rat glioma cells. Cell Growth Differ., *7:* 1175–1186, 1996.
5. Liu, R., Oberley, L. W., and Oberley, T. D. Transfection and expression of MnSOD cDNA decreases tumor malignancy of human oral squamous carcinoma SCC-25 cells. Hum. Gene Ther., *8:* 585–595, 1997.
6. Lebovitz, R. L., Zhang, H., Vogel, H., Cartwright, J., Jr., Dionne, L., Lu, N., Huang, S., and Matzuk, M. M. Neurodegeneration, myocardial injury, and perinatal death in mitochondrial superoxide dismutase-deficient mice. Proc. Natl. Acad. Sci. USA, *93:* 9782–9787, 1996.
7. Orr, W. C., and Sohal, R. S. Extension of life-span by overexpression of superoxide dismutase and catalase in *Drosophila melanogaster*. Science (Wash. DC), *263:* 1128–1130, 1994.
8. Beckman, J. S., Carson, M., Smith, C. D., and Koppenol, W. H. ALS, SOD, and peroxynitrite. Nature (Lond.), *364:* 584, 1993.
9. Chang, L. Y., Slot, J. W., Geuze, H. J., and Crapo, J. D. Molecular immunocytochemistry of the CuZn superoxide dismutase in rat hepatocytes. J. Cell Biol., *107:* 2169–2179, 1988.
10. Marklund, S., Westman, N., Lundgren, E., and Roos, G. Copper- and zinc-containing superoxide dismutase, manganese-containing superoxide dismutase, catalase, and glutathione peroxidase in normal and neoplastic human cell lines and normal human tissues. Cancer Res., *42:* 1955–1961, 1982.
11. Fernandez-Pol, J. A., Hamilton, P. D., and Klos, D. J. Correlation between the loss of the transformed phenotype and an increase in superoxide dismutase activity in a revertant subclone of sarcoma virus-infected mammalian cells. Cancer Res., *42:* 609–617, 1982.
12. Muramatsu, H., Kogawa, K., Tanaka, M., Okumura, K., Nishihori, Y., Koike, K., Kuga, T., and Nitsu, Y. Superoxide dismutase in SAS human tongue carcinoma cell line is a factor defining invasiveness and cell motility. Cancer Res., *55:* 6210–6214, 1995.
13. Tanaka, M., Kogawa, K., Nishinori, Y., Kuribayashi, K., Nakamura, K., Muramatsu, H., Koike, K., Sakamaki, S., and Nitsu, Y. Suppression of intracellular Cu-Zn SOD results in enhanced motility and metastasis of Meth A sarcoma cells. Int. J. Cancer, *73:* 187–192, 1997.
14. Zhong, W., Oberley, L. W., Oberley, T. D., and St. Clair, D. K. Suppression of the malignant phenotype of human glioma cells by overexpression of manganese superoxide dismutase. Oncogene, *14:* 481–490, 1997.
15. Li, N., Oberley, T. D., Oberley, L. W., and Zhong, W. Overexpression of manganese superoxide dismutase in DU145 human prostate carcinoma cells has multiple effects on cell phenotype. Prostate, *35:* 221–233, 1998.
16. Sun, Y., Oberley, L. W., Elwell, J. H., and Sierra-Rivera, E. Lowered antioxidant enzymes in spontaneous transformed embryonic mouse liver cells in culture. Carcinogenesis (Lond.), *14:* 1457–1463, 1993.
17. Spitz, D. R., Elwell, J. H., and Sun, Y. Oxygen toxicity in control and H_2O_2-resistant Chinese hamster fibroblast cell lines. Arch. Biochem. Biophys., *279:* 249–260, 1990.
18. Yan, T., Oberley, L. W., Zhong, W., and St. Clair, D. K. Manganese-containing superoxide dismutase overexpression causes phenotypic reversion in SV40-transformed human lung fibroblasts. Cancer Res., *56:* 2864–2871, 1996.
19. Li, J. J., Domann, F. E., and Oberley, L. W. The use of RT-PCR to distinguish between plasmid MnSOD transcripts and endogenous MnSOD mRNA. Biochem. Biophys. Res. Commun., *216:* 610–618, 1995.
20. Spitz, D. R., and Oberley, L. W. An assay for superoxide dismutase activity in mammalian tissue homogenates. Anal. Biochem., *179:* 8–18, 1989.
21. Beauchamp, C., and Fridovich, I. Superoxide dismutase: improved assays and assay applicable to polyacrylamide gels. Anal. Biochem., *44:* 276–287, 1971.
22. Claiborne, A. Catalase activity. *In:* R. A. Greenwald (ed.), CRC Handbook of Methods for Oxygen Radical Research, pp. 283–284. Boca Raton, FL: CRC Press, Inc., 1985.
23. Gunzler, W., and Flohe, L. Glutathione peroxidase. *In:* R. A. Greenwald (ed.), CRC Handbook of Methods for Oxygen Radical Research, pp. 285–290. Boca Raton, FL: CRC Press, Inc., 1985.
24. Royall, J. A., and Ischiropoulos, H. Evaluation of 2′,7′-dihydrofluorescein and dihydrorhodamine 123 as fluorescent probes for intracellular H_2O_2 in cultured endothelial cells. Arch. Biochem. Biophys., *302:* 348–355, 1993.
25. Kelner, M. J., Bagnell, R. D., Montoya, M. A., Estes, L., Uglik, S. F., and Cerutti, P. Transfection with human copper-zinc superoxide dismutase induces bi-directional alterations in other antioxidant enzymes, proteins, growth factor response, and paraquat resistance. Free Radic. Biol. Med., *18:* 497–506, 1995.

26. Amstad, P., Moret, R., and Cerutti, P. Glutathione peroxidase compensates for the hypersensitivity of Cu. Zn-superoxide dismutase overproducers to oxidant stress. J. Biol. Chem., *269:* 1606–1609, 1994.
27. Michiels, C., Raes, M., Toussaint, O., and Remacle, J. Importance of Se-glutathione peroxidase, catalase and Cu/Zn-SOD for survival against oxidative stress. Free Radic. Biol. Med., *17:* 235–248, 1994.
28. Imlay, J. A., Chin, S. M., and Balazes, R. Toxic DNA damage by hydrogen peroxide through the Fenton reaction *in vivo* and *in vitro*. Science (Wash. DC), *240:* 640–642, 1988.
29. Amstad, P., Peskin, A., Shah, G., Mirault, M. E., Moret, R., Zbinden, I., and Cerutti, P. The balance between Cu,Zn-superoxide dismutase and catalase affects the sensitivity of mouse epidermal cells to oxidative stress. Biochemistry, *30:* 9305–9313, 1991.
30. Elroy-Stein, O., Bagnell, Y., and Groner, Y. Overproduction of human Cu/Zn-superoxide dismutase in transfected cells: extenuation of paraquat-mediated cytotoxicity and enhancement of lipid peroxidation. EMBO J., *5:* 615–622, 1986.
31. Ceballos, I., Delabar, J. M., Nicole, A., Lynch, R. E., Hallewell, R. A., and Sinet, P. M. Expression of transfected human CuZnSOD gene in mouse L cells and NS20Y neuroblastoma cells induces enhancement of glutathione peroxidase activity. Biochem. Biophys. Acta, *949:* 5864–5870, 1988.
32. Kelner, M. J., and Bagnell, R. D. Alternations of endogenous glutathione peroxidase, manganese superoxide dismutase, and glutathione transferase activity in cells transfected with copper-zinc superoxide dismutase expression vector: explanation for variation in paraquat resistance. J. Biol. Chem., *265:* 10872–10875, 1990.
33. Li, S., Yan, T., Yang, J-Q., Oberley, T. D., and Oberley, L. W. The role of cellular glutathione peroxidase redox regulation in the suppression of tumor cell growth by manganese superoxide dismutase. Cancer Res., *60:* 3927–3939, 2000.
34. Rodriguez, A. M., Carrico, P. M., Mazurkiewicz, J. E., and Melendez, J. A. Mitochondrial or cytosolic catalase reverses the MnSOD-dependent inhibition of proliferation by enhancing respiratory chain activity, net ATP production, and decreasing the steady state levels of H_2O_2. Free Radic. Biol. Med., *29:* 801–813, 2000.
35. Yang, J-Q., Li, S., Domann, F. E., Buettner, G. R., and Oberley, L. W. Superoxide generation in v-Ha-*ras*-transduced human keratinocyte HaCaT cells. Mol. Carcinog., *26:* 180–188, 1999.
36. Yang, J-Q., Li, S., Huang, Y., Zhang, H. J., Domann, F. E., Buettner, G. R., and Oberley, L. W. v-Ha-*ras* overexpression induces superoxide production and alters levels of primary antioxidant enzymes. Antioxid. Redox Signaling, *3:* 697–709, 2001.
37. Burdon, R. H., Gill, V., and Rice-Evans, C. Cell proliferation and oxidative stress. Free Radic. Res. Commun., *7:* 149–159, 1989.
38. Burdon, R. H., Gill, V., and Rice-Evans, C. Oxidative stress and tumor cell proliferation. Free Radic. Res. Commun., *11:* 65–76, 1990.
39. Rao, G. N., and Berk, B. C. Active oxygen species stimulate vascular smooth muscle cell growth and proto-oncogene expression. Circ. Res., *70:* 593–599, 1992.

Overexpression of Copper Zinc Superoxide Dismutase Suppresses Human Glioma Cell Growth

Ying Zhang, Weiling Zhao, Hannah J. Zhang, et al.

Cancer Res 2002;62:1205-1212.